Orientational and phase-coexistence behaviour of hard rod-sphere mixtures

ANTYPOV, D. and CLEAVER, D. J. <http://orcid.org/0000-0002-4278-0098>

Orientational and phase-coexistence behaviour of hard rod-sphere mixtures

Dmytro Antypov [1], Douglas J. Cleaver *

Materials Research Institute, Sheffield Hallam University, Pond Street, Sheffield S1 1WB, UK

Abstract

Results are presented from Monte Carlo simulations of bulk mixtures of Hard Gaussian Overlap particles with an aspect ratio of 3:1 and hard spheres with diameters equal to the breadths of the rods. For sphere number-concentrations of 50% and lower, compression of the isotropic fluid results in formation of a homogeneous (i.e. compositionally mixed) nematic phase. The volume fraction of this isotropic-nematic transition is found to increase approximately linearly with sphere concentration. On compression to higher volume fractions, however, this homogeneous nematic phase separates out into coexisting nematic and isotropic phases.

1 Introduction

When simulating or performing a theoretical study on a particular system, it is often informative initially to consider its behaviour in the hard-particle approximation. In this limit, in the canonical ensemble at least, the equilibrium state is determined by the entropy alone [1]. A particular issue that arises when treating mixtures of hard particles is that it is not always straightforward to determine (by theory) or establish (by simulation) whether a given mixture undergoes phase separation. The possibility of fluid-fluid coexistence in binary mixtures of hard spheres with different diameters, for example, has been the focus of several recent studies (see ref. [2] for the current picture). In addition to this system, the competing demixing and ordering behaviours of numerous other binary hard particle mixtures have been studied using both

* Corresponding author. Fax: +44-114-225-3501
Email address: d.j.cleaver@shu.ac.uk (Douglas J. Cleaver).
[1] Present address: Max-Planck-Institut für Polymerforschung, Ackermannweg 10, D-55128 Mainz, Germany.

theory and computer simulation [3–12]. Mixtures of different types of rods [3–5], rods and disks [6,7], and rods and spheres [8–12] have all been investigated. These studies show that, even in the hard-core approximation, binary mixtures can exhibit macroscopic and microscopic demixing as well as orientationally ordered phases.

To date, most theoretical studies of hard rod-sphere mixtures have been restricted to one of two approximations: the rods have been taken either to be thin and noninteracting or to be parallel (*i.e.* perfectly aligned). Experimental studies of the former situation [8] reveal that small thin rods are very efficient depletion agents and readily induce an effective sphere-sphere attraction. A density functional treatment (DFT) of such systems [9], which was restricted to state points where orientational transitions of the rods were not relevant, found only mixed and demixed regions. Another DFT of hard spheres and hard ellipsoids of arbitrary sizes has predicted the coexistence of nematic rod-rich and isotropic sphere-rich phases at high packing fractions [10]. However, the approach adopted in ref.[10] utilised a number of approximations to the rod direct correlation function, which lead to an inadequate description for the behaviour of the nematic order parameter. More recently, the geometrical approximation approach has been used to study entropy driven demixing for the general case of isotropic binary mixtures of convex bodies [5]. Whilst here it was shown that, in general, prolate and oblate particles demix more easily than spherical ones, fluid-fluid demixing of rod-sphere mixtures was found to be explicitly forbidden when the breadths of the rods were made equal to the diameters of the spheres. Like its predecessors, however, this theory did not consider the way in which demixing might be affected by being either preempted or accompanied by an orientational transition of the rods. In contrast, if the rods are kept parallel [11,12], *only* perfectly ordered liquid crystalline behaviour can be studied. In this limit, mixtures of hard spheres and parallel spherocylinders have been shown to form a lamellar phase in which there is microphase separation of the two components. This type of lamellar phase has also been observed for some experimental rod-sphere systems based on suspensions of rod-like viruses and polystyrene spheres [13,14].

Despite this considerable literature, therefore, most of the theoretical approaches used are only truly valid in the limit of very long, thin rods whereas real liquid crystal molecules typically have aspect ratios of 5 or less. For this reason, we present here an exploratory MC simulation study of a hard particle rod-sphere mixture performed using particle shapes and concentrations for which both orientational ordering and demixing are pertinent.

2 Simulation model and results

In this Letter, we present results from MC simulations of mixtures of Hard Gaussian Overlap (HGO) particles with an aspect ratio of 3:1 and hard spheres (HS) with diameters equal to the breadths of the rods. For aspect ratios of 3 and higher, the undiluted HGO model is known to exhibit a density-driven N-I transition; a phase diagram has recently been calculated [15]. In our mixed systems, the interaction between two particles i and j, separated by a distance r_{ij}, is given by

$$U_{ij} = \begin{cases} 0 & (r_{ij} > \sigma_{ij}), \\ \infty & (r_{ij} \leq \sigma_{ij}), \end{cases} \tag{1}$$

where σ_{ij} is the appropriate range parameter function for the particle-type combination, ij. For two hard spheres, σ_{ij} is simply the sphere diameter σ_0. The range parameter function for two HGO particles depends on their orientations, denoted by the unit vectors $\hat{\mathbf{u}}_\mathbf{i}$ and $\hat{\mathbf{u}}_\mathbf{j}$, and is given by [16]

$$\sigma(\hat{\mathbf{r}}_\mathbf{ij}, \hat{\mathbf{u}}_\mathbf{i}, \hat{\mathbf{u}}_\mathbf{j}) = \sigma_0 \left[1 - \frac{\chi}{2} \left\{ \frac{(\hat{\mathbf{r}}_\mathbf{ij} \cdot \hat{\mathbf{u}}_\mathbf{i} + \hat{\mathbf{r}}_\mathbf{ij} \cdot \hat{\mathbf{u}}_\mathbf{j})^2}{1 + \chi(\hat{\mathbf{u}}_\mathbf{i} \cdot \hat{\mathbf{u}}_\mathbf{j})} + \frac{(\hat{\mathbf{r}}_\mathbf{ij} \cdot \hat{\mathbf{u}}_\mathbf{i} - \hat{\mathbf{r}}_\mathbf{ij} \cdot \hat{\mathbf{u}}_\mathbf{j})^2}{1 - \chi(\hat{\mathbf{u}}_\mathbf{i} \cdot \hat{\mathbf{u}}_\mathbf{j})} \right\} \right]^{-1/2}, \tag{2}$$

where $\hat{\mathbf{r}}_\mathbf{ij} = \mathbf{r}_\mathbf{ij}/r_{ij}$ is the unit vector along the intermolecular vector $\mathbf{r}_\mathbf{ij}$ and $\chi = (k^2 - 1)/(k^2 + 1)$, k being the particle aspect ratio. For un-like particles, for example, if particle i is a sphere and particle j is a rod, σ_{ij} is given by [16]

$$\sigma(\hat{\mathbf{r}}_\mathbf{ij}, \hat{\mathbf{u}}_\mathbf{j}) = \sigma_0 \left[1 - \chi(\hat{\mathbf{r}}_\mathbf{ij} \cdot \hat{\mathbf{u}}_\mathbf{j})^2 \right]^{-1/2}. \tag{3}$$

All simulations were performed in the constant NVT ensemble using a standard MC algorithm. For each trial move, a particle was selected at random and subjected to a random trial displacement within a cube centred on the particle's original position. Where the selected particle was a rod, this displacement was combined with a random rotation implemented using the Barker-Watts method [17]. N such random MC moves made up one MC cycle, so that, on average, each particle experienced one trial move per cycle.

Five HGO-HS systems were simulated, the sphere concentrations being 0%, 10%, 20%, 30%, 40% and 50%, by number. The total number of particles was kept at $N = 2048$ for all systems, the numbers of rods and spheres being adjusted to provide each desired concentration. A compression sequence was performed at each concentration, each sequence starting from a low density, orientationally isotropic configuration. The orientational order parameter was

calculated as the ensemble average of the largest eigenvalue of the Q tensor:

$$Q_{\alpha\beta} = \frac{1}{N_{\rm rod}} \sum_{i=1}^{N_{\rm rod}} \frac{1}{2}(3u_{i\alpha}u_{i\beta} - \delta_{\alpha\beta}), \tag{4}$$

where $N_{\rm rod}$ is the number of rods in the system, $u_{i\alpha}$ is the α component ($\alpha = x, y, z$) of the vector $\hat{\mathbf{u}}_\mathbf{i}$, and $\delta_{\alpha\beta}$ is the Kronecker delta. The mean square particle displacement was also monitored routinely to ensure that, within each run, the particles travelled distances comparable with the simulation box side; had the runs been significantly shorter than this, it would have been impossible to assess any possible demixing occurring in the system. This requirement lead to run-lengths of between 6×10^5 and 1.5×10^7 MC cycles, depending on the system density.

Fig. 1 shows the nematic order parameter as a function of occupied volume fraction at various sphere concentrations. Here, we follow theoretical treatments of HGO systems [18,19] in equating the volume of an HGO particle with that of an ellipsoid of the same elongation. The occupied volume fraction can then be expressed in terms of the total number density $\rho = \frac{N}{V}$ and the sphere number-concentration ratio $0 \leq c_{\rm sph} \leq 1$ using

$$f = \frac{V_{\rm occupied}}{V} \approx \frac{V_{\rm sph}\left(N_{\rm sph} + 3N_{\rm rod}\right)}{V} = \rho V_{\rm sph}\left(3 - 2c_{\rm sph}\right), \tag{5}$$

where $N_{\rm sph}$ is the number of spheres in the system, and $V_{\rm sph}$ and $3V_{\rm sph}$ are the sphere and rod volumes, respectively. The data shown in Fig. 1 indicate that an N-I transition occurred during each compression sequence. The data also show a clear tendency for the volume fraction at the transition, $f_{\rm N-I}$, to increase with increasing sphere concentration. At the highest sphere concentration studied, 50%, the volume fraction at which the N-I transition occurred was so great that the mobility of the particles was very low: 1.5×10^7 MC cycles were required to equilibrate the last configuration in this compression sequence. Sphere concentrations above 50% were not studied because of this dramatic increase in the required computational time.

The structural behaviour exhibited during compression of the 50% mixture was studied by monitoring the sphere-sphere radial distribution function $g_{\rm ss}(r)$. The difference between the short-range regions of $g_{\rm ss}(r)$ for the 50% mixture above and below $f = 0.53$ is indicative of phase separation (Fig. 2). A configuration snapshot taken at $f = 0.534071$, shown in Fig. 3, confirms this assessment; it shows a rod-rich phase, almost free of spheres, coexisting with a rod-sphere mixture with a high (about 70%) concentration of spheres. This suggests that the volume fraction at which phase separation takes place depends only weakly on sphere concentration, especially at $0 \leq c_{\rm sph} \leq 0.50$.

For the 50% system, it is not clear whether a brief window of homogeneous nematic stability preceded this phase-separation; the latter appears to have taken place at a slightly higher volume fraction than the rise seen in the nematic order parameter, but the volume-fraction difference is similar to the density increments used. In order to assess this more fully, the 20% mixture was compressed to similarly high volume fractions to investigate its phase-separation behaviour. The resulting $g_{\rm ss}(r)$ curves, shown in Fig. 4, indicate a weak but growing tendency for the spheres to cluster with increase in system density, but approach unity at large r for all volume fractions considered. This suggests a random distribution of small clusters of spheres. A number and size distribution analysis of clusters of spheres separated by distances greater than $1.5\sigma_0$ was performed at each density and averaged over at least 10^5 MC cycles. The resulting data, which are shown in Tab. I, indicate that macroscopic phase separation was not seen: about a hundred clusters of spheres (half of which were just single spheres) were found even at the highest density. That said, the largest cluster contained about 20% of the total number of spheres at high densities.

Since the runs performed here were sufficiently long to give an average net sphere displacement greater than the simulation box side, these systems were certainly not glassy. Also, the clusters of spheres were found to change dynamically during the runs. When compared with the results from the 50:50 system simulations, phase separation would have been expected at about the same volume fraction, i.e. $f = 0.53$. This is consistent with the point at which the size of the largest cluster started to increase significantly (Tab. I). We also note a possible anomaly in the gradient of the order parameter curve of the 20% mixture at this volume fraction. These observations both suggest that the 20% mixture may have a weak tendency to phase separate. Our inability directly to observe macroscopic phase coexistence here is not surprising, however; finite size effects, particularly the relatively high surface to volume ratio of a sphere-rich droplet at low overall sphere concentrations, would be expected to inhibit such an observation in a constant NVT simulation. Finally, we note that the order parameter values shown in Tab. I increase at a volume fraction of about 0.50, indicating that a compositionally homogeneous nematic phase was present in the range $0.50 < f < 0.53$. This supports the possibility of there being a similar but much narrower window of homogeneous nematic stability in the 50% mixture.

3 Discussion and Conclusion

The simulations presented here show that, while binary mixtures of hard spheres and HGO particles with aspect ratio 3 do not exhibit lamellar structures, they do undergo macroscopic phase separation at high volume fraction.

A partial phase diagram for the system is shown in Fig. 5, diamonds representing the simulation points. Here, the dashed line connects points at which the increase of the nematic order parameter indicates a N-I phase transition. It was not possible to resolve the individual isotropic and nematic coexistence densities from our exploratory NVT simulations. However, the weakly first-order nature of the N-I transition dictates that the dashed line in Fig. 5 actually represents a narrow region of N+I coexistence. We also indicate, with a solid line, the approximate location of the much wider, re-entrant N+I coexistence region identified from our simulations at high volume fractions. We note that an equivalent wide N+I coexistence region has been seen at low T in the temperature-concentration phase diagram of a liquid crystal-silicone oil mixture [20]. It has also been seen in lattice model simulations of thermotropic liquid crystal-isotropic fluid mixtures [21,22].

In discussing these results further, there are two useful reference points to consider: the random close packing volume fraction $f_{\rm HSF} \simeq 0.64$ (the short dashed line in Fig. 5) and the freezing point of a monodisperse hard sphere system [23], $f_{\rm HSF} \simeq 0.494$ (the dot-dashed line). In rod-sphere mixtures with low sphere concentrations, an N-I transition occurs at volume fractions below $f_{\rm HSF}$. At these sphere concentrations, the ordered phase is simply a nematic containing randomly dispersed spheres, *i.e.* the mixing entropy is high. As the concentration of spheres is increased, the N-I transition shifts towards progressively higher volume fractions before, at a sphere concentration slightly over 50%, the narrow coexistence region associated with the homogeneous N-I transition opens up into a very broad N+I coexistence envelope which dominates for volume fractions above $f \approx 0.53$. The simulation method we have used is not able either to access the (presumably glassy and crystalline) structures pertaining at very high volume fractions or determine the boundaries of the N+I coexistence envelope at low and high sphere concentrations. We do not, therefore, speculate on these areas of the phase diagram.

In a pure hard-rod system, the N-I transition point is determined by the balance of the (orientational and rotational) ideal-gas and excluded volume entropy terms. On extending this $c_{\rm sph} = 0.0$ limit to two-component rod-sphere mixtures, the excluded volume term splits into three separate elements (rod-rod, sphere-sphere and rod-sphere), while the mixing entropy is introduced by expressing the ideal gas contributions from each component with separate terms. For these systems, the excluded volume contributions which significantly influence the N-I transition are the rod-rod and rod-sphere terms: the increase in $f_{\rm NI}$ with sphere concentration simply indicates that these excluded volume terms drop more rapidly than the orientational ideal-gas contribution as the number of rods in the system is reduced. In contrast, it is competition between the mixing entropy and the various excluded volume contributions that determines the boundary of the re-entrant N+I phase coexistence region. On leaving the homogeneous nematic region, the system sacrifices its mixing

entropy in order to reduce the weight given to the rod-sphere excluded volume term and increase those given to the more efficient rod-rod and sphere-sphere contributions.

In conclusion, our simulation results have shown that this simple hard-particle mixture exhibits both an orientational ordering transition and a re-entrant N+I phase-coexistence region which occupies a significant concentration range at high volume fractions. Having established the generic behaviour of rod-sphere mixtures in the hard particle approximation, our future work will explore the changes brought to this base phase diagram by the introduction of attractive interactions with various symmetries.

Acknowledgements

This work has benefitted greatly from numerous discussions with Chris Care. We also gratefully acknowledge the financial support of the MRI in providing a studentship for D.A., and EPSRC for providing computational hardware under grant GR/L86135.

References

[1] D. Frenkel, Physica A 263 (1999) 26

[2] M. Dijkstra, R. van Roij, R. Evans, Phys. Rev. E, 59 (1999) 5744

[3] A. Stroobants, Phys. Rev. Letts. 69 (1992) 2388

[4] R. van Roij, B. Mulder, Phys. Rev. E 54 (1996) 6430

[5] H. Bosetti and A. Perera, Phys. Rev. E 63 (2001) 021206

[6] A. Galindo, G. Jackson, and D.J. Photinos, Chem. Phys. Letts. 325 (2000) 631

[7] P.J. Camp, M.P. Allen, Physica A 229 (1996) 410

[8] K. Lin, J.C. Crocker, A.C. Zeri, A.G.Yodh, Phys. Rev. Letts. 87 (2001) 088301

[9] M. Schmidt, Phys. Rev. E 63 (2001) 050201

[10] A. Samborski and G. T. Evans, J. Chem. Phys. 107 (1994) 6005

[11] T. Koda, M. Numajiri, and S. Ikeda, J. Phys. Soc. Jpn. 65 (1996) 3551

[12] Z. Dogic, D. Frenkel and S. Fraden, Phys. Rev. E 62 (2000) 3925

[13] M. Adams and S. Fraden, Biophys. J. 74 (1998) 669

[14] M. Adams, Z. Dogic, S.L. Keller, and S. Fraden, Nature 393 (1998) 349

[15] E. de Miguel and E. Martín del Río, J. Chem. Phys. 115 (2001) 9072

[16] B.J. Berne and P. Pechukas, J. Chem. Phys. 64 (1972) 4213

[17] J.A. Barker and R.O. Watts, Chem. Phys. Letts. 3 (1969) 144

[18] M. Rigby, Mol. Phys. 68 (1989) 687

[19] P. Padilla and E. Velasco, J. Chem. Phys. 106 (1997) 10299

[20] J.C. Loudet, P. Barois and P. Poulin, Nature 407 (2000) 611

[21] R. Hashim, G.R. Luckhurst and S. Romano, Proc. Roy. Soc Lond A 429 (1990) 323

[22] M.A. Bates, Phys. Rev. E 64 (2001) 051702

[23] M.D. Rintoul, S. Torquato, Phys. Rev. E 58 (1998) 532

Table I. Order parameter and cluster distribution measured for the 80/20 mixture at different volume fractions f.

f	Order parameter	Number of clusters	Largest cluster
0.490015	0.206 ± 0.023	188.4 ± 6.6	16.7 ± 3.8
0.496821	0.486 ± 0.012	167.8 ± 7.7	21.4 ± 8.3
0.503626	0.568 ± 0.018	164.3 ± 7.2	21.1 ± 6.3
0.510432	0.609 ± 0.010	159.9 ± 6.0	18.6 ± 4.5
0.517238	0.655 ± 0.011	139.8 ± 9.5	37.4 ± 12.8
0.524044	0.695 ± 0.007	123.7 ± 5.9	39.6 ± 8.3
0.530850	0.723 ± 0.007	115.7 ± 8.9	61.9 ± 15.2
0.537655	0.742 ± 0.010	120.9 ± 5.8	42.4 ± 10.8
0.544461	0.771 ± 0.012	107.2 ± 6.2	88.2 ± 21.6
0.551267	0.795 ± 0.006	79.5 ± 4.5	80.8 ± 22.4
0.558073	0.806 ± 0.004	79.7 ± 5.3	66.5 ± 12.6

Figure 1. Order parameter dependence on volume fraction for various mixtures.

Figure 2. Sphere-sphere radial distribution functions measured in 50% mixture at different volume fractions.

Figure 3. Configuration snapshot of 50/50 mixture taken at volume fraction $f = 0.534071$.

Figure 4. Sphere-sphere radial distribution functions measured in 20% mixture at different volume fractions.

Figure 5. Approximate phase diagram of our hard particle mixture.

Figure. 1

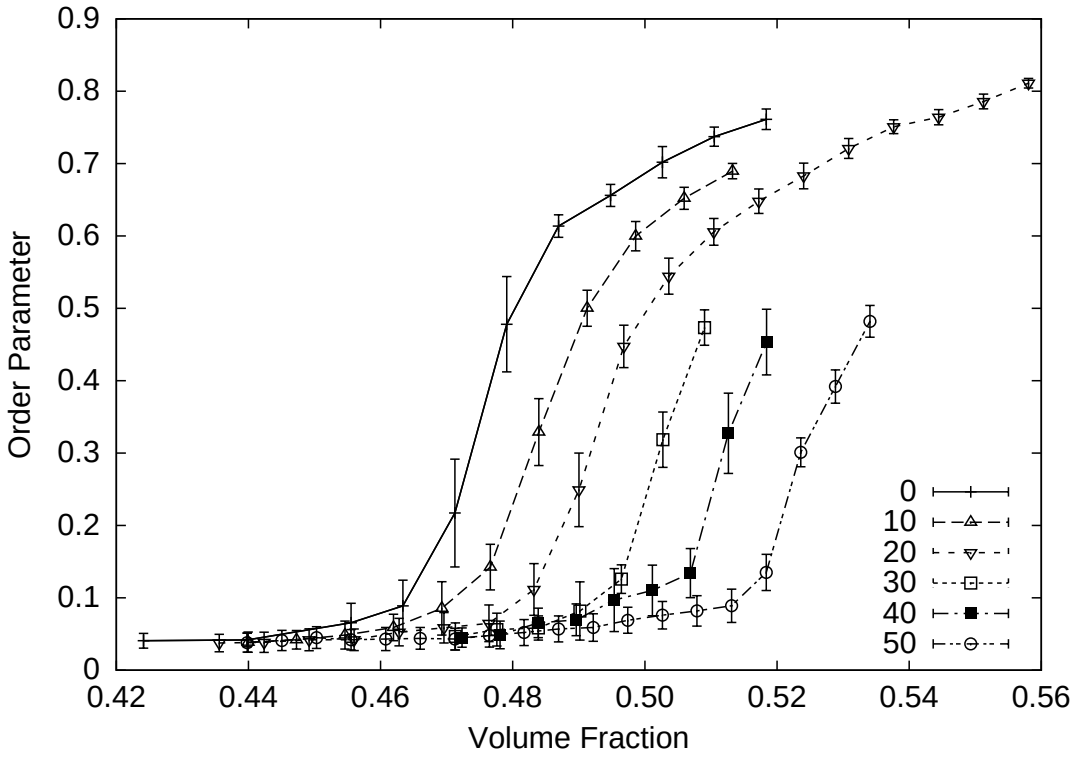
Order Parameter
Volume Fraction
0.9
0.8
0.7
0.6
0.5
0.4
0.3
0.2
0.1
0
0.42
0.44
0.46
0.48
0.50
0.52
0.54
0.56
0
10
20
30
40
50

Figure. 2

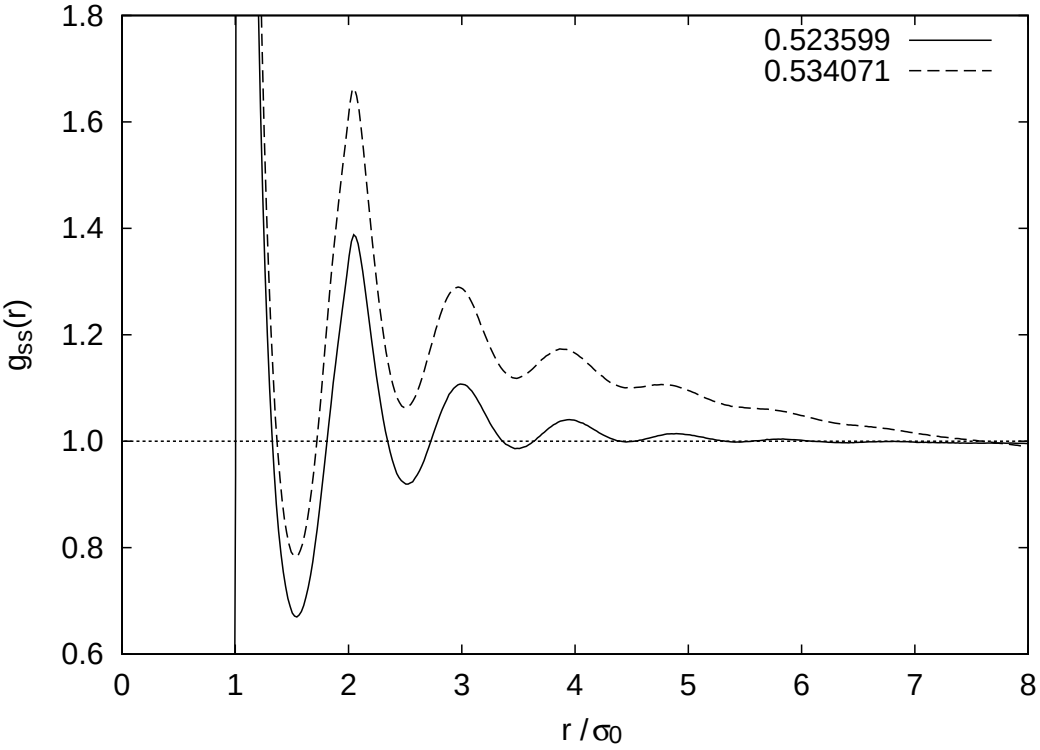

Figure. 3

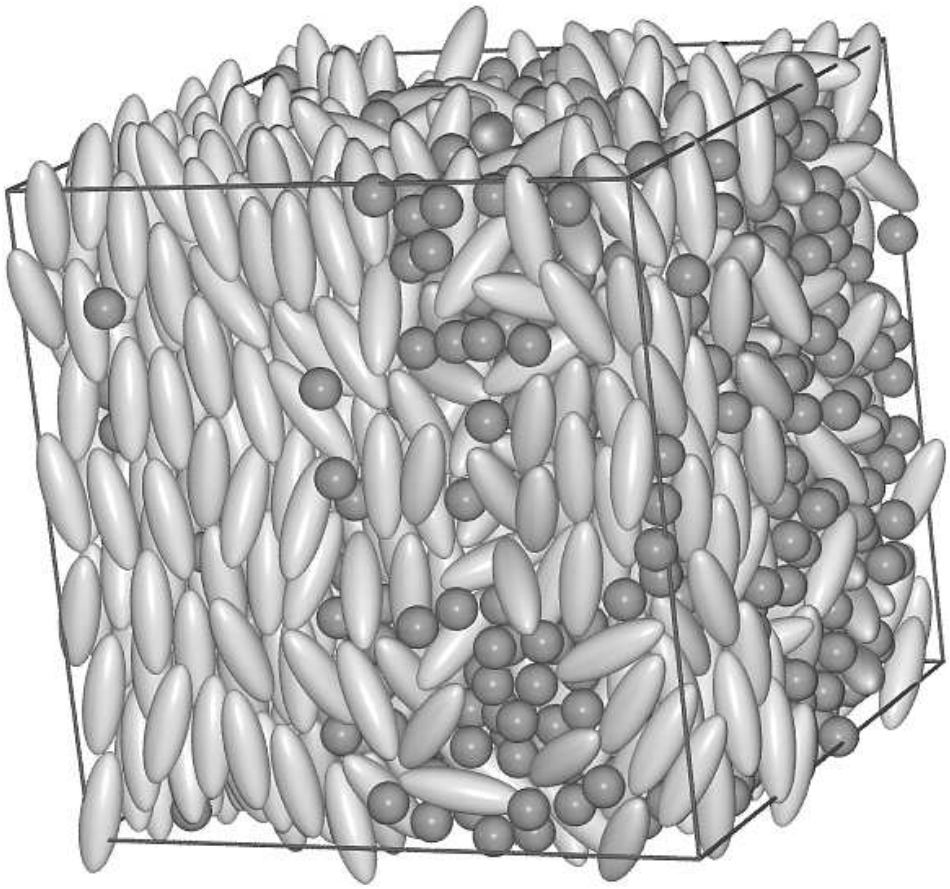

Figure. 4

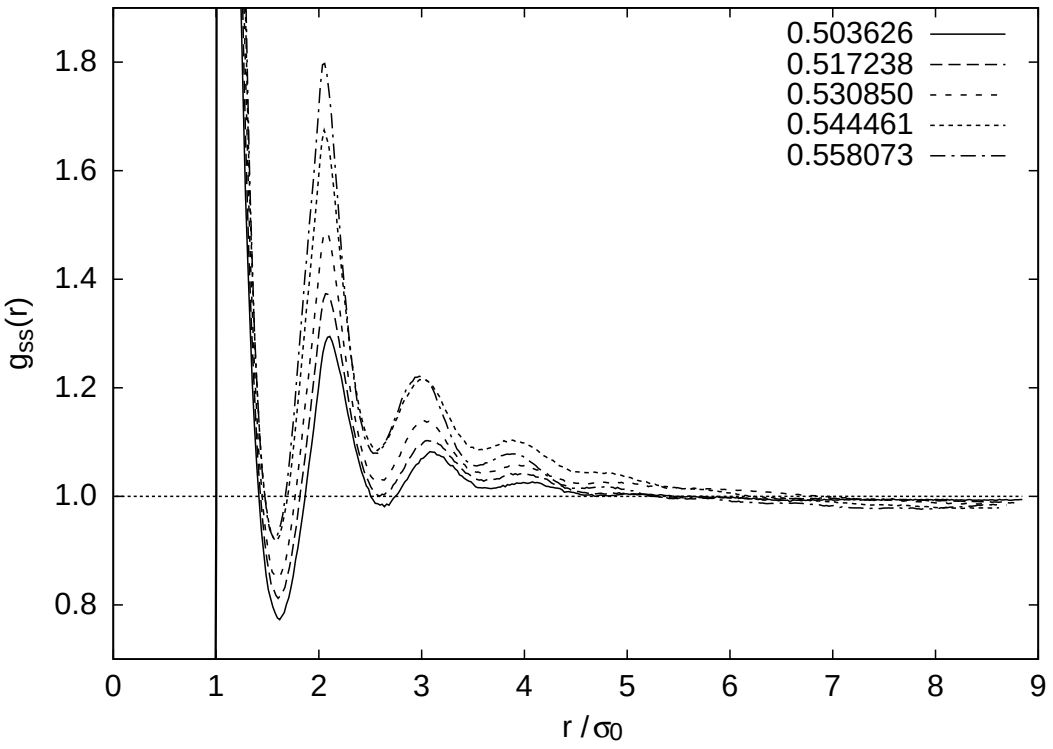
0.503626
0.517238
0.530850
0.544461
0.558073
1.8
1.6
1.4
1.2
1.0
0.8
$g_{ss}(r)$
0
1
2
3
4
5
6
7
8
9
r / σ_0

Figure. 5

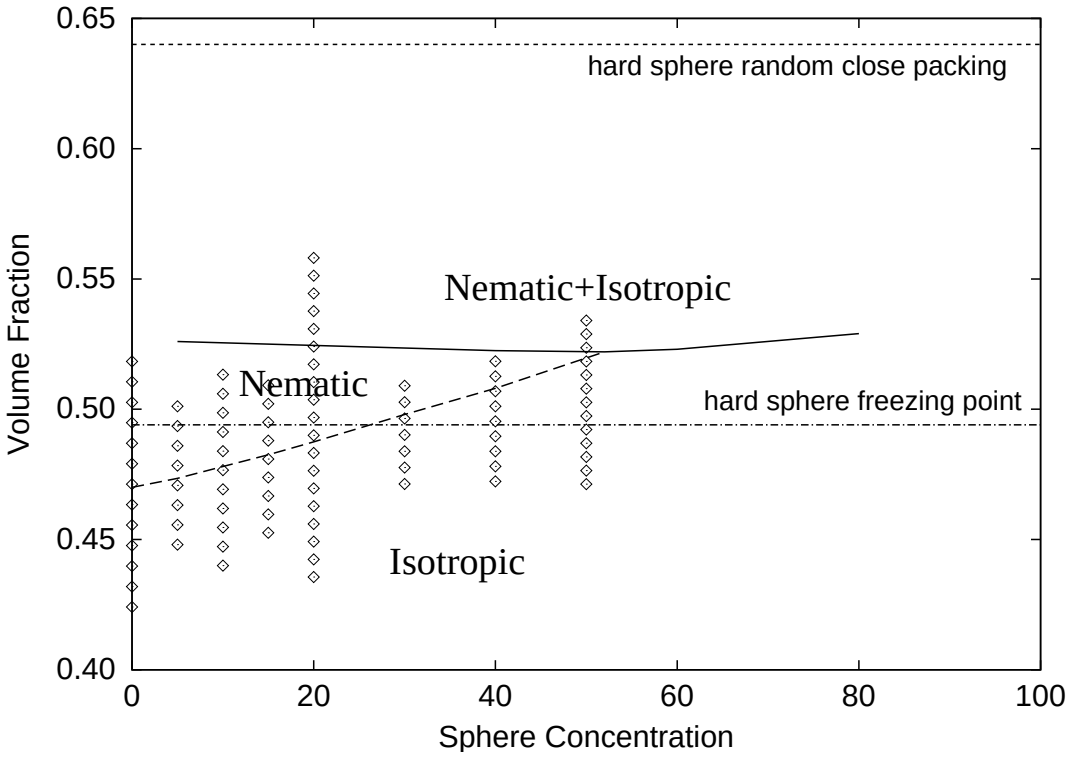
0.65
0.60
0.55
0.50
0.45
0.40
Volume Fraction
hard sphere random close packing
Nematic+Isotropic
Nematic
hard sphere freezing point
Isotropic
0
20
40
60
80
100
Sphere Concentration